

# OCR evaluation of cohesionless soil in centrifuge model using shear wave velocity

Hyung Ik Cho<sup>1a</sup>, Chang Guk Sun<sup>1b</sup>, Jae Hyun Kim<sup>2c</sup> and Dong Soo Kim<sup>\*3</sup>

<sup>1</sup>Earthquake Research Center, Korea Institute of Geoscience and Mineral Resources,  
124 Gwahak-ro, Yuseong-gu, Daejeon 34132, Republic of Korea

<sup>2</sup>Department of Infrastructure Safety Research, Korea Institute of Civil Engineering and Building Technology,  
283 Goyangdae-ro, Goyang-si, Gyeonggi-do 10223, Republic of Korea

<sup>3</sup>Department of Civil Engineering, Korean Advanced Institute of Science and Technology,  
291 Daehak-ro, Yuseong-gu, Daejeon 34141, Republic of Korea

(Received June 21, 2017, Revised December 4, 2017, Accepted January 8, 2018)

**Abstract.** In this study, a relationship between small-strain shear modulus ( $G_{max}$ ) and overconsolidation ratio ( $OCR$ ) based on shear wave velocity ( $V_S$ ) measurement was established to identify the stress history of centrifuge model ground. A centrifuge test was conducted in various centrifugal acceleration levels including loading and unloading sequences to cause various stress histories on centrifuge model ground. The  $V_S$  and vertical effective stress were measured at each level of acceleration. Then, a sensitivity analysis was conducted using testing data to ensure the suitability of  $OCR$  function for the tested cohesionless soils and found that  $OCR$  can be estimated based on  $V_S$  measurements irrespective of normally-consolidated or overconsolidated loading conditions. Finally, the developed  $G_{max}$ - $OCR$  relationship was applied to centrifuge models constructed and tested under various induced stress-history conditions. Through a series of tests, it was concluded that the induced stress history on centrifuge model by compaction, g-level variation, and past overburden load can be analysed quantitatively, and it is convinced that the  $OCR$  evaluation technique will contribute to better interpret the centrifuge test results.

**Keywords:** overconsolidation ratio ( $OCR$ ); shear wave velocity ( $V_S$ ); centrifuge tests

## 1. Introduction

The stress condition subjected to a soil element is one of the most important factors that affect the behavior of soils. Since soil elements of in-situ ground are subjected to anisotropic loading condition incorporating the stress history by natural or sometimes artificial process, the effect of stress history on the behavior of soils has been investigated by many studies. The stress states of soil elements can be expressed in terms of overconsolidation ratio ( $OCR$ ) value representing the stress history. The  $OCR$  value is the ratio of the maximum overburden pressure in the past ( $\sigma'_p$ ) and the present vertical effective pressure ( $\sigma'_v$ ), which characterizes the stress history effect. Clayton *et al.* (1985) reported that effect of overconsolidation under zero lateral yield ( $K_O$ ) conditions, which might be broadly interpreted in the field, has two important effects on a soil: (a) the yield surface is expanded, so that reload deformation

is reduced, and (b) the horizontal stresses are increased above their normally consolidated  $K_O$  level.

The in-situ penetration test is a practical method for the indirect prediction of soil properties (Duman *et al.* 2014, Zhang and Goh 2016). Many design parameters are converted from the results of penetration tests such as SPT- $N$ , CPT- $q_c$  values, and those values are affected by the stress history of soil deposits. The major effect of the stress history on in-situ test results is due to the increase in the horizontal stress level (Clayton *et al.* 1985, Lee *et al.* 2011). Skempton (1986) reported the effect of stress history on the increase of the SPT- $N$  value due to effective preconsolidation pressure ( $\sigma'_p$ ). Lee *et al.* (2011) also studied the effect of stress history on the results of CPT and DMT tests for granular soils. Although the relative density and current stress level are the most influential factors on in-situ test results, the stress history also plays an important, albeit secondary, role (Clayton *et al.* 1985, Lee *et al.* 2011). To sum up, given that many geotechnical design parameters are determined from the results of penetration tests, which depend on the stress history, design methods and construction costs can be significantly influenced according to the in-situ  $OCR$  value.

The determination of effective preconsolidation pressure ( $\sigma'_p$ ) and corresponding  $OCR$ , which define the stress history of soil, through laboratory tests is difficult because of sample disturbance. In particular, granular soil samples used in the laboratory tests have experienced greater disturbance and stress release than cohesive soils during

\*Corresponding author, Professor

E-mail: [dskim@kaist.ac.kr](mailto:dskim@kaist.ac.kr)

<sup>a</sup>Ph.D.

E-mail: [hicho@kigam.re.kr](mailto:hicho@kigam.re.kr)

<sup>b</sup>Ph.D.

E-mail: [pungsun@kigam.re.kr](mailto:pungsun@kigam.re.kr)

<sup>c</sup>Ph.D.

E-mail: [jaehyun@kict.re.kr](mailto:jaehyun@kict.re.kr)

sampling procedures, and, therefore, laboratory tests cannot fully represent the in-situ stress state. The consequence is that the pre-consolidation pressure is always underestimated (Jamiolkowski *et al.* 1985). Although a sampling technique of sand specimen using freezing method has been proposed (Yoshimi *et al.* 1978, Goto *et al.* 1992), it has not been widely used due to technical problems such as the need for prior research on the change in engineering properties of the sample by freezing and thawing and the accompanying cost problems.

It is also difficult to evaluate *OCR* of centrifuge model ground even though many centrifuge tests are performed using an overconsolidated centrifuge model. In order to make the overconsolidated model, the pre-consolidation pressure is applied on the model by the vertical loading system before the model container is placed on the centrifuge arm so that the design *OCR* can be simulated at the target *N g*-level (Afacan *et al.* 2013, Choo *et al.* 2013). As another method, by spinning the centrifuge at the higher *g*-levels than the target *g*-level, the model can be experienced maximum past pressure before doing the planned testing at the lower target *g*-level (Hu *et al.* 2011, Adalier and Elgamal 2005, El-Sekelly *et al.* 2015). Although the efforts have been made for *OCR* simulation designed in the testing plan, the evaluation of real-simulated *OCR* is not performed at the target *g*-level. For obtaining the *OCR*, the conventional laboratory testing methods have to be conducted after centrifuge simulation by sampling the centrifuge model. In this case, the sample also experiences the same problems likewise the laboratory tests as aforementioned. The centrifuge model ground, inevitably, involves the stress history during model ground construction, seating the model box on basket and centrifuge testing including staged tests by changing acceleration levels. Even though the centrifuge test provides a well-controlled event with known boundary conditions, unavoidable uncertainty, which can disturb the planned stress condition, is included in the model ground due to such reasons. Therefore, the stress history of the model ground in terms of *OCR* should be carefully considered in the analysis.

In this study, a relationship between small-strain shear modulus ( $G_{max}$ ) and *OCR* based on shear wave velocity ( $V_S$ ) measurement is established to identify the effect of the stress history on centrifuge model in terms of *OCR*. The  $G_{max}$ -*OCR* relationship is determined especially for cohesionless soils which are commonly utilized as a constructing material of centrifuge model in many centrifuge centres. In order to validate the relationship, a centrifuge test was conducted in various centrifugal acceleration levels including loading and unloading sequences to cause various stress histories on centrifuge model ground. Then, a sensitivity analysis was conducted using testing data to ensure the suitability of *OCR* function for the tested cohesionless soils. Finally, the developed  $G_{max}$ -*OCR* relationship was applied to centrifuge models constructed and tested under various induced stress-history conditions such as compaction, *g*-level variation, and past overburden load.

## 2. *OCR* effect on $G_{max}$ for cohesionless soils

The small-strain shear modulus,  $G_{max}$ , is directly related

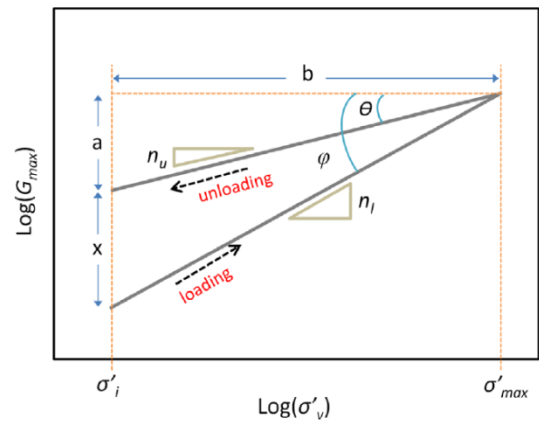


Fig. 1 Typical variation in  $G_{max}$  during loading and unloading for the model of *OCR* exponent estimation:  $\sigma'_i$  = initial effective vertical stress;  $\sigma'_{max}$  = maximum effective vertical stress;  $n_u$  = stress exponent during unloading;  $n_l$  = stress exponent during loading (Choo and Burns 2014)

to the average effective principal stresses in the direction of wave propagation and in the direction of particle motion while the  $G_{max}$  is independent of the magnitude of normal stress on the plane through which the shear body wave propagates (Roesler 1979, Knox *et al.* 1982, Yu and Richart 1984). This suggests the use of  $\sigma'_o = (\sigma'_1 + \sigma'_3)/2$ , instead of mean principal stress, in Eq. (1) when the soil is subjected to an anisotropic stress state (Shibuya *et al.* 1997). The  $G_{max}$  is also a function of void ratio ( $e$ ) of the soil and *OCR* value for cohesive soil, and can be expressed by the well-known Hardin and Richart equation taking the general form as follows

$$G_{max} = A \cdot F(e) \cdot (\sigma'_o)^n \cdot OCR^k \quad (1)$$

where,  $A$  = an experimentally determined constant reflecting soil fabric;  $n$  = an experimentally determined exponent, approximately equals to 0.5;  $\sigma'_o = (\sigma'_v + \sigma'_h)/2$  kPa, where  $\sigma'_v$  is vertical effective stress and  $\sigma'_h$  is horizontal effective stress;  $k$  = exponent of *OCR* value that increases from 0 to 0.5 as the plasticity index increases from 0 to 100 (Hardin and Drnevich 1972), which means that *OCR* has no effect on  $G_{max}$  for cohesionless soils;  $e$  is void ratio and  $F(e)$  is void ratio function. According to Lopresti (1989), the  $F(e)$  can be given by

$$F(e) = e^{-1.3} \quad (2)$$

Considering the coefficient of earth pressure at rest ( $K_o$ ), Eq. (1) can be modified to

$$G_{max} = A \cdot F(e) \cdot \left( \frac{(1 + K_o)\sigma'_v}{2kPa} \right)^n OCR^k \quad (3)$$

Since the *OCR* exponent  $k$  is zero for the cohesionless soils, the Eq. (1) is revised to

$$G_{max} = A \cdot F(e) \cdot \left( \frac{\sigma'_v}{2kPa} \right)^n (1 + K_o)^n \quad (4)$$

Application of the *OCR* term on the  $G_{max}$  equation is suitable for cohesive soils to account the stress history

effect. In case of cohesionless soils, since the current stress condition affected by stress history is represented by only the horizontal stress variation (i.e.,  $K_0$ ) in the stress term (Eq. (4)), the  $OCR$  exponent  $k$  in Eq. (1) is negligible as mentioned above. On the other hands, if the  $G_{max}$  for the cohesionless soils is expressed employing only the vertical effective stress as the stress term, instead of average effective stress, the Eq. (1) could be rewritten as

$$G_{max} = A' \cdot F(e) \cdot \left( \frac{\sigma_v'}{1 \text{ kPa}} \right)^n OCR^{k'} \quad (5)$$

In this case, the  $OCR$  function can be accounted to represent the current stress condition including the stress history effect as  $OCR$  even for cohesionless soils. Based on the geometry of Fig. 1 and Eq. (5), the slope of the loading and unloading curves can be determined, geometrically (Hryciw and Thomann 1993, Choo and Burns 2014). The  $OCR$  exponent  $k'$  in Eq. (5) can be obtained by

$$k' = n_l - n_u \quad (6)$$

From Eq. (6), it is clear that  $OCR$  exponent  $k'$  in Eq. (5) is equivalent to the difference between the stress exponents in loading and unloading. This means that the  $OCR$  exponent  $k'$  reflects the increment of horizontal stress caused by lateral stress locked during unloading stage.

### 3. Sensitivity analysis by centrifuge test

If Eq. (5) is utilized in determination of  $G_{max}$  for cohesionless soils, the suitability of  $OCR$  function in the equation should be examined in advance. Even though the variables  $(1+K_0)^n$  in Eq. (4) and  $OCR^{k'}$  in Eq. (5) represent the effect of horizontal stress on  $G_{max}$  identically, the Eq. (5) is not equal to Eq. (4) analytically. Sensitivity analysis was performed to validate the role of  $OCR^{k'}$  substituting that of  $(1+K_0)^n$  in the  $G_{max}$  equation for cohesionless soils using centrifuge test results. A centrifuge test was carried out using a uniformly constructed centrifuge model. Here, testing setup was described briefly. A pair of bender elements and an earth pressure transducer were utilized for measurements of  $V_S$  and earth pressure of the model (Kim and Kim 2010, Youn *et al.* 2008). The bender elements has been widely used in the centrifuge experiments to measure the  $V_S$  due to their simplicity, low cost, and non-destructive testing characteristics (El-Sekelly *et al.* 2014, Kim *et al.* 2017). The bender elements was installed at a depth of 37.7 cm from model ground surface as cross-hole type configuration, and the distance between corresponding bender tips was 15 cm. The earth pressure transducer was installed on the bottom of model box. The measured vertical effective stresses were planned to be linearly interpolated for obtaining the vertical effective stress at the depth of the bender elements. The model ground was uniformly prepared by air pluviation using dry silica sand. The relative density of the prepared ground was 70% and the height of the soil model was 47.7 cm. The centrifuge test was carried out under various acceleration g-levels in steps. The centrifuge model was accelerated to 70 g, then decelerated to 10 g using 10 g steps. The  $V_S$  and earth pressure were

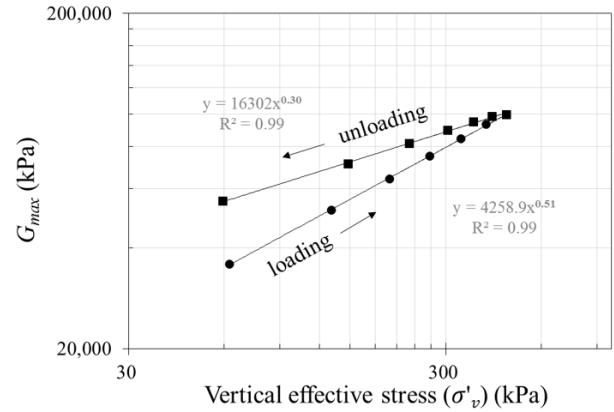


Fig. 2 Variation in  $G_{max}$  during the loading and unloading using measured vertical effective stress

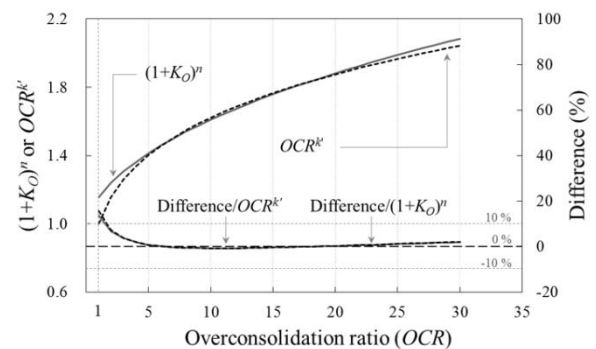


Fig. 3 The effects of  $(1+K_0)^n$  and  $OCR^{k'}$  terms on  $G_{max}$  equation for silica sand

measured at each 10 g increment and decrement.

In this study,  $V_S$  was calculated using the tip-to-tip distance between two corresponding bender elements and the first arrival time by peak-to-peak method using data obtained during the centrifuge test. Because the peak-to-peak method was utilized with an input motion of 5 kHz sinusoidal signal, which is a high enough input frequency, the reliability of  $V_S$  determination was ensured (Yamashita *et al.* 2009). In addition, note that the 5 kHz input motion and travel distance of 15 cm resulted in an adequate travel distance-to-wavelength ratio ( $R_d^{in}$ ) within a range of 2 to 4 assuming  $V_S$  of 200 m/s for the tested sand, and this means that the degree of scatter in stiffness measurements (i.e.,  $V_S$ ) is smallest in this range (Yang and Gu 2013) by avoiding the near field effect (El-Sekelly *et al.* 2013). Then, the  $G_{max}$  relationship could be established for the tested silica sand. Firstly, the  $G_{max}$  is calculated from the obtained  $V_S$  as:

$$G_{max} = \rho \cdot V_S^2 \quad (7)$$

where,  $\rho$  is the mass density of the soil. Secondly, the stress exponents for loading and unloading conditions can be determined using the  $G_{max}$  and measured vertical effective stress as shown in Fig. 2. The stress exponents  $n_l$  of 0.51 for loading and  $n_u$  of 0.30 for unloading were determined respectively for the silica sand. Finally, the  $OCR$  exponent  $k'$ , which equals to the difference between those stress exponents, was obtained as 0.21. The obtained stress exponent  $n_u$  is closer to the theoretically derived stress

exponent  $1/3$ , while the stress exponent  $n_l$  equals to approximately  $1/2$ , as most previous experimental studies have reported (Choo and Burns 2014). The reason of markedly lower stress exponent  $n$  for  $G_{max}$  for unloading stages can be explained by the decrease in effective stress. When stresses are reduced during unloading stages, the contact stiffness decreases. Thus, if constant fabric is assumed, the coordination number decreases when effective confining stresses decrease, and this leads to the decrease in stress exponent  $n$  (Cho *et al.* 2006).

The effect of the variations in  $(1+K_o)^n$  of Eq. (4) and  $OCR^{k'}$  of Eq. (5) on  $G_{max}$  were analysed with respect to the  $OCR$  from 1 to 30 as presented in Fig. 3. Mayne and Kulhawy's (1982) equation for unloading was adopted to calculate the  $K_o$  as follows

$$K_o = (1 - \sin\phi) \cdot OCR^{\sin\phi} \quad (8)$$

where,  $\phi$  is the friction angle. The friction angle of  $42^\circ$ , which is corresponding to relative density of 70 %, was obtained by the triaxial tests and applied (Kim *et al.* 2015). The stress exponent  $n$  of 0.51 measured during loading sequence was adopted for calculation of the  $(1+K_o)^n$  because the effect of horizontal stress increase on  $G_{max}$  by stress history is accounted by only  $K_o$  increase. In the Fig. 3, the comparison shows that  $(1+K_o)^n$  and  $OCR^{k'}$  deduce almost similar values over  $OCR$  of 3 while there is small discrepancies for the region less than  $OCR$  of 3. The degree of difference against the  $(1+K_o)^n$  and  $OCR^{k'}$  is also expressed as a percentage in the figure. The both differences are less than  $\pm 10\%$  in the  $OCR$  range of 3 to 30. In particular, it can be confirmed that the difference is close to zero in the region over  $OCR$  of 5. Therefore, it could be concluded that the  $OCR^{k'}$  could replace the role of  $(1+K_o)^n$  in  $G_{max}$  estimation for cohesionless soils, although there is small difference in the region less than  $OCR$  of 3.

#### 4. Application of the $G_{max}$ - $OCR$ relationship to various centrifuge models

##### 4.1 Establishment of the $G_{max}$ - $OCR$ relationship for silica sand

Centrifuge model ground, inevitably, contains the stress history during testing procedures. The stress history of model ground could be obtained in terms of  $OCR$  if the  $G_{max}$ - $OCR$  relationship was established for testing soil materials. In this section, the  $G_{max}$ - $OCR$  relationship was established for the silica sand. The silica sand used in this study is clean sand and artificially produced by crushing quartzite (Kim *et al.* 2015). Fig. 4 shows the particle shapes of the silica sand taken by an optical microscope. The particle size distribution of the silica sand is compared with other sand materials as present in Fig. 5. The silica sand could be regarded as a medium grained sand and its basic properties are shown in Table 1.

The centrifuge test results explained in previous section such as measured  $V_s$  and earth pressure could be utilized in the determination of the  $G_{max}$ - $OCR$  relationship for the silica sand. In addition to determined stress exponent  $n$  and  $OCR$  exponent  $k'$ , the constant  $A'$  in Eq. (5) need to be

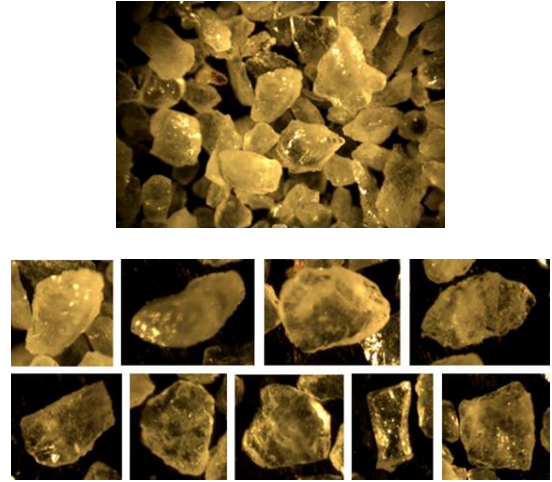


Fig. 4 Particle shapes of silica sand taken by an optical microscope

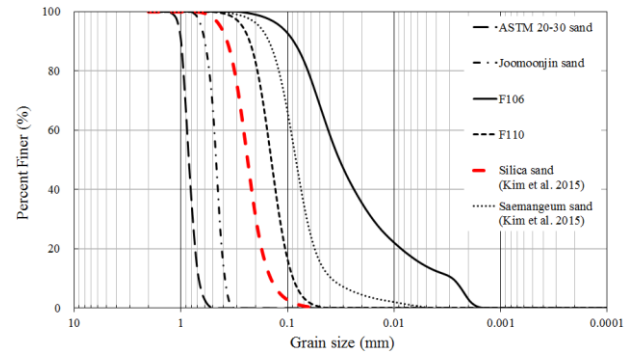


Fig. 5 Comparison of particle size distribution of silica sand with other sand materials

Table 1 Basic physical properties of silica sand

Properties	Parameters
Soil classification, USCS	SP
Specific gravity, $G_s$	2.65
Fine contents passing #200 (%)	0.9
Maximum dry density ( $t/m^3$ )	1.64
Minimum dry density ( $t/m^3$ )	1.24
$D_{10}$ (mm)	0.148
$D_{50}$ (mm)	0.237
$D_{60}$ (mm)	0.257
Coefficient of uniformity, $C_u$	1.60
Plastic index, $PI$	NP

calculated using the void ratio function of  $e^{-1.3}$ , which was addressed in Eq. (2), based on the measured  $V_s$  and earth pressure values. The  $V_s$  and earth pressure values, which were obtained during the first loading stage, were adopted so as to make the  $OCR$  equals to 1. Fig. 6 presents the relationship between  $G_{max}$  normalized by vertical effective stress and void ratio according to the established  $G_{max}$  relationship based on the Eq. (5). The test results for the

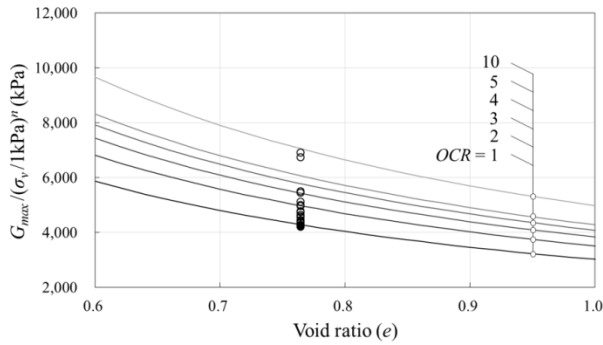


Fig. 6 Relationship between normalized  $G_{max}$  and void ratio of the silica sand

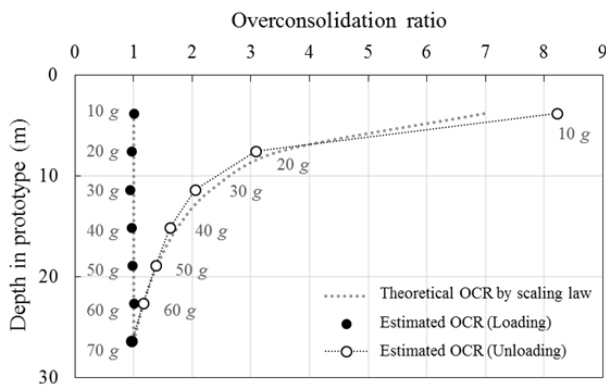


Fig. 7 Comparison of the  $OCR$  values from the  $G_{max}$ - $OCR$  relationship and scaling law

loading and unloading cycle are plotted on the figure, and compared with the established curves that vary with  $OCR$ . Because the  $G_{max}$  is normalized by the vertical effective stress, the variation of the data in vertical axis represents the effect of horizontal stress increment over the normally consolidated condition. Consequently, the effect of the horizontal stress increase can be directly related to  $OCR$  according to Eq. (5). Open circles indicate the data obtained during unloading condition of the model ground (70 g to 10 g) while the solid circles mean the data obtained during normally consolidated condition (10 g to 70 g). Note that no change in void ratio was assumed during loading cycles.

The  $OCR$  values estimated on the Fig. 6 are demonstrated with expected depths of  $V_s$  measurements in prototype as shown in Fig. 7. In addition, the  $OCR$  evaluated by the  $G_{max}$ - $OCR$  relationship is compared with that calculated theoretically using the depth of bender element installation, unit weight of the silica sand and target  $g$ -level based on centrifuge scaling law (Tasiopoulou *et al.* 2015). It can be noted that the  $OCR$  values estimated by the  $G_{max}$  -  $OCR$  relationship show good agreements with that from the scaling law. As expected, it is possible to check the stress history of centrifuge model ground in terms of  $OCR$  quantitatively even for the cohesionless soil.

#### 4.2 Application to centrifuge models with various testing conditions

The centrifuge models experience the stress history during testing procedures such as model ground

Table 2 Comparisons of centrifuge models and testing conditions that cause stress history

	Case 1	Case 2	Case 3	Case 4	Case 5
Model construction method	Compaction*	Pluviation	Pluviation	Pluviation	Pluviation
Target $g$ -level (g)	Single (40)	Multi (10-20-30-50-70-50*-30*)	Single (40)	Multi* (10-20-30-40-50-60-70-60*-50*-40*-30*-20*-10*)	Multi* (20-30-50-70-30*)
Surcharge load application	X	X	O*	X	X
Model box dimension (cm)	Square (100x100x47.7 by width by length by height)	Cylindrical (90x70 by diameter by height)	Square (100x100x47.7 by width by length by height)	Square (100x100x47.7 by width by length by height)	Cylindrical (90x70 by diameter by height)
Model thickness (cm)	46	45	47.7	46	45
Depth(s) of $V_s$ measurement by bender elements (cm)	Various (6 to 30 in 2 intervals)	Various (6 to 28 in 2 intervals)	Various (6 to 30 in 2 intervals)	Single (37.7)	Various (6 to 28 in 2 intervals)
Void ratio ( $e$ )	#1 0.677 #2 0.688 #3 0.692	#1 0.704	#1 0.737 #2 0.744	#1 0.764	#1 0.926

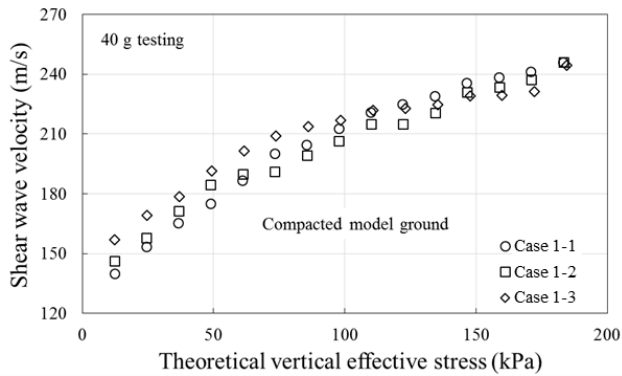
\*Causes of stress history on each centrifuge model

construction, seating the model box on basket, staged tests by changing  $g$ -levels and additional load application on the model during the test. In case of simple centrifuge tests performed at various  $g$ -levels using the same model, the stress history effect can be predicted by the centrifuge scaling law with depth theoretically as verified in previous section. However, it is difficult to estimate the stress history of model ground for somewhat complicated tests. In this section, the  $G_{max}$ - $OCR$  relationship established for the silica sand is applied for various centrifuge models.

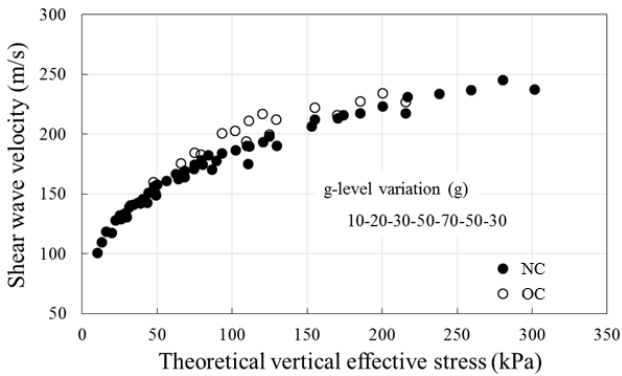
In Table 2, the information of centrifuge model grounds, which were constructed and tested under various testing conditions, is shown for the comparison. The centrifuge models are divided into 5 groups. Each group is classified based on the testing conditions that induce different stress history on the models such as construction method, target  $g$ -level variation and surcharge load application during the centrifuge test. All of centrifuge tests were performed using dry silica sand, and the centrifuge test, which was mentioned in section 3, is assigned as Case 4. The centrifuge models of Case 1 were constructed at 1 g level by dry compaction method. In this case, it is difficult to estimate the stress state of model at the target  $g$ -level due to the effect of compaction energy at 1 g. In case of Case 3, additional surcharge load was applied and removed on model ground surface at single target  $g$ -level by vertical loading system. The stress history of Case 2, Case 4 and Case 5 was induced by  $g$ -level changing identically to see the effect of void ratio of wide range. Furthermore, three and two models of Case 1 and Case 3 were constructed and tested, respectively, under the identical testing condition having slightly different void ratios. The buried depth(s) of bender elements from the soil surface and  $g$ -level variation in each experiment simulated various prototype depths according to the centrifuge scaling law. The bender elements tests were conducted at the centre part of model to minimize the arching effect caused by box wall.

Fig. 8 shows  $V_s$  obtained from centrifuge tests with vertical effective stress for each model. Since earth pressure

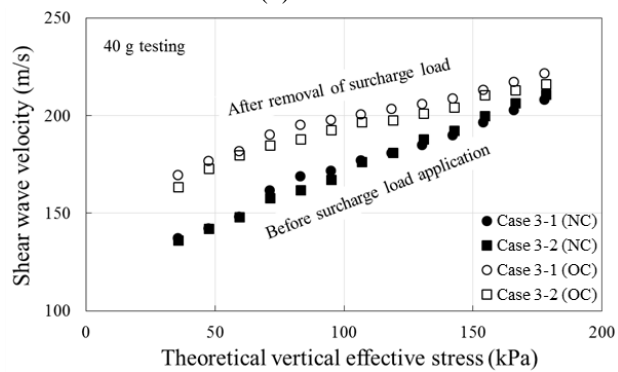
transducers were not installed within model grounds except the Case 4, the vertical effective stresses were calculated theoretically based on scaling law. As mentioned before, it is assumed that there is no arching effect, which causes



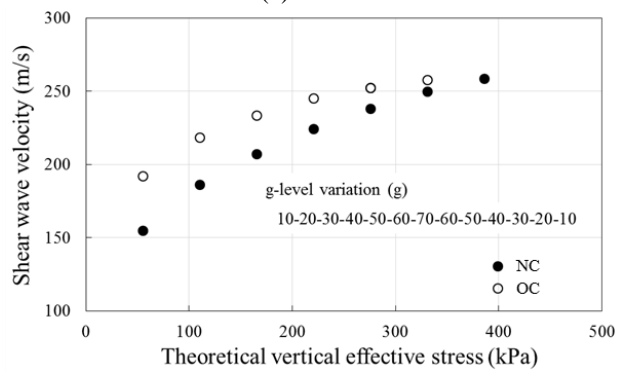
(a) Case 1



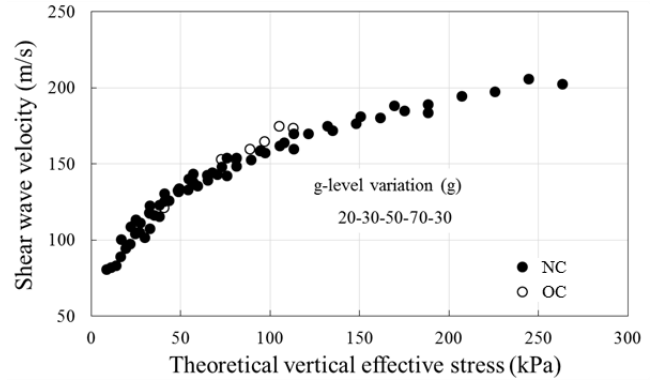
(b) Case 2



(c) Case 3



(d) Case 4



(e) Case 5

Fig. 8 Continued

reduction in vertical effective stress, at centre (Cho *et al.* 2014). Except the Case 1, which the centrifuge model was constructed by compaction at 1 g, the data are expressed as open circles for normal loading condition or solid circles for overconsolidated loading condition. Because the quantitative comparison is not possible between the compaction energy applied at 1 g and the stress increments due to the *g*-level increase on the model at the target *g*-level, the data points for Case 1 were presented as open circles. With the exception of Case 1, it can be seen that  $V_S$  values obtained from overconsolidated loading condition are higher than those from normal loading condition at the same vertical effective stress conditions.

#### 4.3 OCR Evaluation of various centrifuge models

The degree of horizontal stress increment caused by overconsolidated loading conditions was analysed with the  $G_{max}$ -OCR relationship curves using the  $V_S$  measurements as shown in Fig. 9. The parameters  $A'$ ,  $n$  and  $k'$  in Eq. (5) for the sand used in this study was utilized in the analysis. It is assumed that void ratio was not changed during testing procedures because the effect of centrifugal acceleration on settlements of model was insignificant as increase in relative density ranged from 0.2% (the highest density case) to 6% (the lowest density case). In Case 1-3, the void ratio is adjusted to the right to avoid overlapping of the data because the void ratio is very similar to that of Case 1-2. Since the theoretical vertical effective stress is applied instead of the measured vertical effective stress as with the other results, there is small difference between the results of Case 4 and those in Fig. 6.

In Fig. 9, solid circles are resulted from  $V_S$  values obtained for normally consolidated loading condition while open circles indicates the results from those obtained for overconsolidated loading condition as presented in Fig. 6.

Because the centrifuge models were constructed by air-pluviation method except Case 1 and further the  $V_S$  measurements were attempted before additional-surcharge load application or *g*-level variation to lower levels, which cause the stress history on centrifuge model grounds, the solid points have to be close to the curve having OCR of 1 (NC line). In Case 1, since inherent stress history was already contained due to compaction energy at 1 g, the data

Fig. 8 Measured shear wave velocities with theoretical vertical effective stress

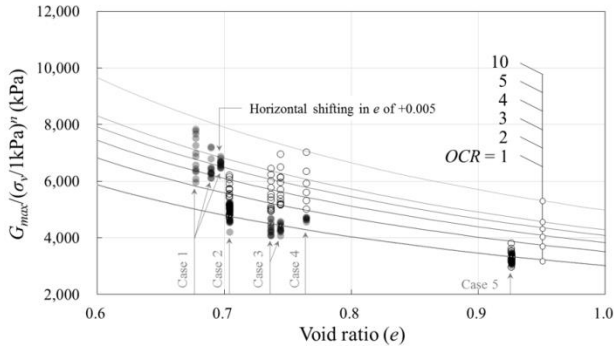
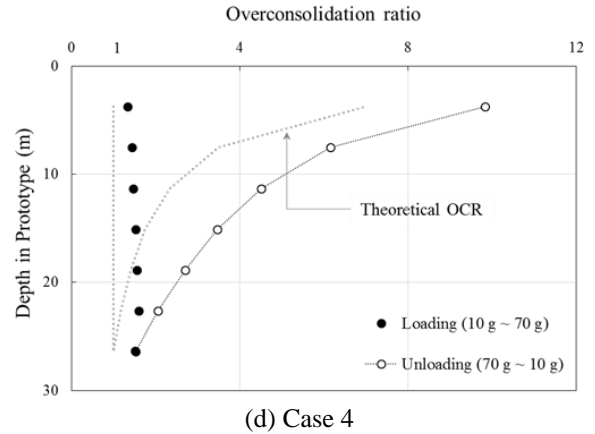
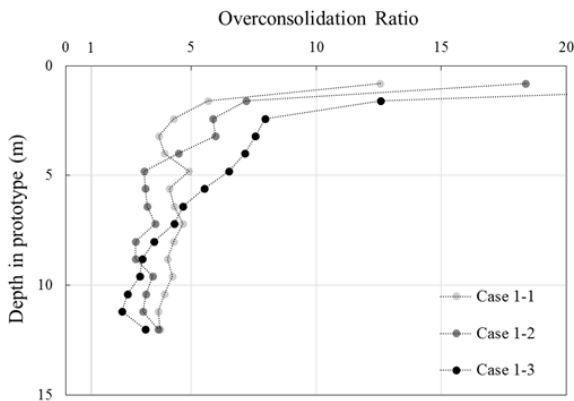


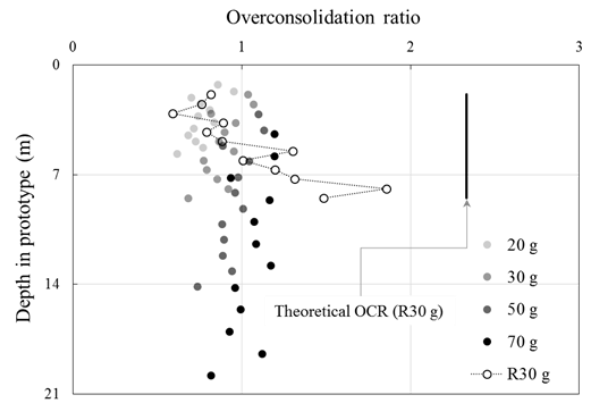
Fig. 9 Relationship between normalized  $G_{max}$  and void ratio ( $e$ ) for centrifuge models constructed and tested under various conditions using this silica sand



(d) Case 4

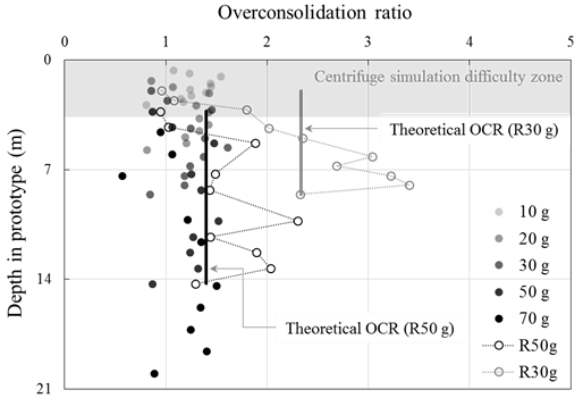


(a) Case 1

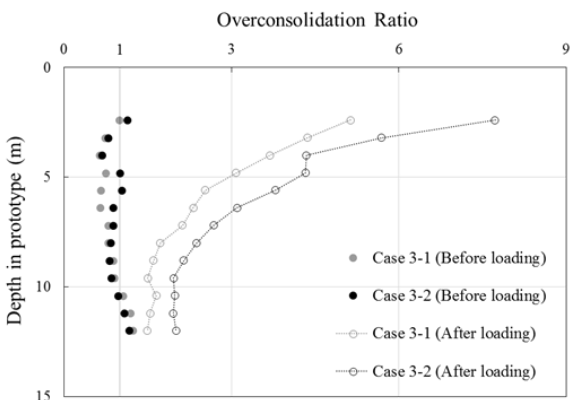


(e) Case 5

Fig. 10 Continued



(b) Case 2



(c) Case 3

Fig. 10 Estimated OCR with prototype depth, (a) Case 1, (b) Case 2, (c) Case 3, (d) Case 4, and (e) Case 5

was distributed above the NC line even at target  $g$ -level of 40  $g$ . However, the solid circles from Case 2, 3, 4 and 5 show also some discrepancies with the NC curve. In addition to the use of the theoretical vertical effective stresses in Eq. (5), the other possible reason can be attributed to the use of  $OCR^k$  in the  $G_{max}$  equation. This could result in small error near the NC line as discussed in section 3. However, the errors do not exceed the curve having OCR of 2.

Open circles indicate the data obtained from overconsolidated loading conditions. For Case 1, it can be seen that stress history due to compaction energy at 1  $g$  affects the stress state of the model during  $N$   $g$  centrifuge tests. Three centrifuge models of Case 1, which were constructed and tested under same conditions but different void ratios, resulted in scattering on the figure. Although same degree of compaction was intended for the three models, experimental errors or heterogeneity caused during model preparation is unavoidable. This confirms that the  $G_{max}$ -OCR relationship is appropriate in uniformity evaluation of the centrifuge model ground. The open circles from Case 2, 4 and 5 show the effect of stress history caused by  $g$ -level variation. The OCR variation of Case 2 and 5 is smaller than that of Case 4, because degree of  $g$ -level variations is lesser as shown in Fig. 8. In Case 3, loading and unloading of surcharge load were applied on the surface of the centrifuge model up to 2600 kPa for Case 3-1 and 3000 kPa for Case 3-2, respectively. Therefore, it is possible to investigate the effect of stress history induced by

past surcharge load on subsurface stress state.

The  $OCR$  values of each centrifuge model are determined according to the data points on Fig. 9, and it is presented with prototype depth as shown in Fig. 10. Centrifuge models of Case 1, which were tested under single 40  $g$ -level, show higher  $OCR$  values at shallow depths while the  $OCR$  values decrease as the depth becomes deeper for three models. Since high centrifugal acceleration at target  $g$ -level makes the model ground has  $N$  times higher stress condition by the scaling law, the effect of compaction energy at 1  $g$  decreases as the depth becomes deeper. In Case 2, the centrifuge model experienced stress history by  $g$ -level variation and the  $V_S$  was measured at various depths. Because the various depths of the  $V_S$  measurements simulate various prototype depths even at certain  $g$ -level, the estimated  $OCR$  values are presented with  $g$ -level, separately. The evaluated  $OCR$  values are scattered around  $OCR$  of 1 but less than  $OCR$  of 2 in the loading condition from 10  $g$  to 70  $g$ . As mentioned earlier, it is discussed that the  $OCR^k$  term used in the  $G_{max}$ - $OCR$  relationship results in a slight error in the normally consolidated state. The  $OCR$  values derived from overconsolidation loading condition at the level of 50  $g$  and 30  $g$  (i.e., the model that experienced 70  $g$ ) show larger values than those derived from the normally consolidated state and average values are similar to the theoretical value presented as solid lines. The scattering is considered as an inevitable experimental error caused during model preparation such as construction, moving and seating the model box on the centrifuge basket. However, small values near  $OCR = 1$  are derived for the shallow depth, which is attributed to the fact that the shallow depth of the centrifugal model does not properly simulate the actual stress level. Kim *et al.* (2017) reported that the differences of  $V_S$  between loading and unloading conditions are less than 2 % at the shallow depth (less than 3 m in prototype). Furthermore, given that  $OCR$  values evaluated for Case 3, which was conducted with additional surcharge load application on the surface during the test, are significantly higher even at shallow depths due to residual stress caused by the overburden load, it is clear that centrifuge modelling does not adequately simulate the stresses in shallow depths especially for uniformly constructed models. The  $OCR$  values estimated for two centrifuge models of Case 3 show similar tendency each other after removing the surcharge load while the absolute values are slightly different with depth because the level of the surcharge loads was different. Large  $OCR$  values are observed at shallow depth due to overburden loading, and the  $OCR$  decreases with depth and this tendency is consistent with Boussinesq's theory. It is meaningful to quantitatively evaluate this effect in terms of the  $OCR$ . It is expected that the  $OCR$  evaluation technique will make the study possible about the transition process of the surcharge load to the subsoil layer. Conversely, it would be also possible to estimate the maximum previous load through the  $OCR$  evaluation. The results of Case 4 discussed in Section 3 are shown in Fig. 10 (d). Unlike the results on Fig. 7, theoretically calculated vertical effective stress was applied to the  $OCR$  evaluation. Since the measured vertical effective stress includes the experimental errors occurred during the model preparation, the  $OCR$  evaluation with higher accuracy can be accomplished by using the measured vertical effective stress. Nevertheless, the trend of  $OCR$

values evaluated at unloading stages is also similar to that of the theory with difference at most  $OCR$  of 2. Case 5 is an experiment almost identical with Case 2, but with a large void ratio and the results are similar to those of Case 2 at normal loading stages. The  $OCR$  values at unloading stage of 30  $g$  are smaller than theoretical ones and this can be attributed to the stress simulation problem of shallow depth in the centrifuge test as described above. Given that the horizontal stress increase, which is one of major effects of stress history, by locked-in stresses around the individual soil particles is minimal in loose sand condition than dense condition (Kim *et al.* 2017), it is found that the stress state change due to the  $g$ -level variation is insignificant at shallow depths below 5 m in prototype scale in the loose density condition.

The  $G_{max}$ - $OCR$  relationship could be adopted in in-situ investigation. As discussed in introduction, the  $OCR$  affects the behavior of soil, and the results of in-situ penetration tests and various-related engineering properties are influenced by stress history of ground. Even though this research has been limited to centrifugal tests, it could be expected that if the parameters  $A'$ ,  $n$  and  $k'$ , which are required in the  $G_{max}$ - $OCR$  relationship, were determined by laboratory test such as an oedometer test, the in-situ  $OCR$  could be quantified by combining the relationship with field seismic test results. Once the  $OCR$  values are obtained, maximum previous load that makes serious effect on compressibility of soils could be evaluated.

## 5. Conclusions

In this study, the stress history of centrifuge model was investigated in terms of  $OCR$  based on the  $G_{max}$  -  $OCR$  relationship. The  $G_{max}$  -  $OCR$  relationship was developed especially for silica sand. Sensitivity analysis was performed to validate the developed relationship. Finally, centrifugal models were constructed and tested under various testing conditions that induce stress history effect on the centrifuge model. The following results are obtained:

1) A  $G_{max}$ - $OCR$  relationship was developed for cohesionless soils using  $OCR^k$  term substituting  $(1+K_O)^n$  in general  $G_{max}$  equation. The validity of the  $G_{max}$ - $OCR$  relationship was verified by sensitivity analysis using centrifuge test results. The results showed that the difference between  $OCR^k$  and  $(1+K_O)^n$  was less than 10%.

2) Centrifuge model tests were performed using dry silica sand for various testing conditions. The causes of stress history on centrifuge model were identified as  $g$ -level variation, surcharge load application during  $N$   $g$  centrifuge testing, and model construction by compaction at 1  $g$ . Total 5 cases were tested with wide void ratio range of model ground.

3) The  $OCR$  values could be evaluated quantitatively according to the established  $G_{max}$ - $OCR$  relationship based on  $V_S$  measurements irrespective of normally-consolidated (NC) or overconsolidated (OC) loading conditions of various models. The estimated  $OCR$  values were slightly scattered near the  $OCR$  of 1 due to the effect of  $OCR^k$  term in the  $G_{max}$ - $OCR$  relationship for the normally consolidated loading state with experimental errors. In particular, the  $OCR$  evaluation can be accomplished with higher accuracy

by using the measured vertical effective stress.

4) The  $OCR$  values estimated by the  $G_{max}$ - $OCR$  relationship revealed that the centrifuge test does not properly simulate the actual stress at shallow depths during unloading stages especially for the model having loose relative density. To sum up, the  $G_{max}$ - $OCR$  relationship shows great feasibility for broad range of void ratio, and it is confirmed that the  $OCR$  of centrifuge models could be well quantified based on the relationship.

## Acknowledgements

This research was supported from Basic Research Project of Korea Institute of Geoscience and Mineral Resources (KIGAM). Also, support from the National Research Foundation of Korea (NRF) grant funded by the Korea government (MSIT) (No. 2017R1A5A1014883) was acknowledged.

## References

- Afacan, K.B., Brandenberg, S.J. and Stewart, J.P. (2013), "Centrifuge modeling studies of site response in soft clay over wide strain range", *J. Geotech. Geoenviron. Eng.*, **140**(2), 04013003.
- Cho, G.C., Dodds, J. and Santamarina, J.C. (2006), "Particle shape effects on packing density, stiffness, and strength: natural and crushed sands", *J. Geotech. Geoenviron. Eng.*, **132**(5), 591-602.
- Cho, H.I., Park, H.J., Kim, D.S. and Choo, Y.W. (2014), "Evaluation of  $K_O$  in centrifuge model using shear wave velocity", *Geotech. Test. J.*, **37**(2), 255-267.
- Choo, H. and Burns, S.E. (2014), "Effect of overconsolidation ratio on dynamic properties of binary mixtures of silica particles", *Soil Dyn. Earthq. Eng.*, **60**, 44-50.
- Choo, Y.W., Kim, J.H., Park, H.I. and Kim, D.S. (2012), "Development of a new asymmetric anchor plate for prefabricated vertical drain installation via centrifuge model tests", *J. Geotech. Geoenviron. Eng.*, **139**(6), 987-992.
- Clayton, C.R.I., Hababa, M.B. and Simons, N.E. (1985), "Dynamic penetration resistance and the prediction of the compressibility of a fine-grained sand-a laboratory study", *Geotechnique*, **35**(1), 19-31.
- Duman, E.S., Ikipler, S.B., Angin, Z. and Demir, G. (2014), "Assessment of liquefaction potential of the Erzincan, Eastern Turkey", *Geomech. Eng.*, **7**(6), 589-612.
- El-Sekelly, W., Abdoun, T. and Dobry, R. (2015), "Effect of overconsolidation on  $K_O$  in centrifuge models using CPT and tactile pressure sensor", *Geotech. Test. J.*, **38**(2), 150-165.
- El-Sekelly, W., Mercado, V., Abdoun, T., Zeghal, M. and El-Ganainy, H. (2013), "Bender elements and system identification for estimation of  $V_S$ ", *J. Phys. Model. Geotech.*, **13**(4), 111-121.
- El-Sekelly, W., Tessari, A. and Abdoun, T. (2014), "Shear wave velocity measurement in the centrifuge using bender elements", *Geotech. Test. J.*, **37**(4), 1-16.
- Goto, S., Suzuki, Y., Nishio, S. and Ohoka, H. (1992), "Mechanical properties of undisturbed Tone-river gravel obtained by in-situ freezing method", *Soil. Found.*, **32**(3), 15-25.
- Hardin, B.O. and Drnevich, V.P. (1972), "Shear modulus and damping in soils: Measurement and parameter effects", *J. Soil Mech. Found. Div.*, **98**(sm6).
- Hryciw, R.D. and Thomann, T.G. (1993), "Stress-history-based model for  $G^e$  of cohesionless soils", *J. Geotech. Eng.*, **119**(7), 1073-1093.
- Hu, H.J.E., Leung, C.F., Chow, Y.K. and Palmer, A.C. (2011), "Centrifuge modelling of SCR vertical motion at touchdown zone", *Ocean Eng.*, **38**(7), 888-899.
- Jamiolkowski, M. (1985), "New developments in field and laboratory testing of soil", *Proceedings of the 11th International Conference on Soil Mechanics*, San Francisco, California, U.S.A., August.
- Kim, J.H., Cho, H.I., Park, H.J. and Kim, D.S. (2017), "Evaluation of soil state variation using bender elements within centrifuge models", *Geotech. Test. J.*, **40**(1), 150-159.
- Kim, J.H., Choo, Y.W., Kim, D.J. and Kim, D.S. (2015), "Miniature cone tip resistance on sand in a centrifuge", *J. Geotech. Geoenviron. Eng.*, **142**(3), 04015090.
- Kim, N.R. and Kim, D.S. (2010), "A shear wave velocity tomography system for geotechnical centrifuge testing", *Geotech. Test. J.*, **33**(6), 434-444.
- Knox, D.P., Stokoe, K.H.I and Kopperman, S.E. (1982), *Effect of State of Stress in Velocity of Low Amplitude Shear Waves Propagating along Principal Stress Directions in Dry Sand*, No. GR82-23, Texas University at Austin Geotechnical Engineering Center, Austin, Texas, U.S.A.
- Lee, M.J., Choi, S.K., Kim, M.T. and Lee, W.J. (2011), "Effect of stress history on CPT and DMT results in sand", *Eng. Geol.*, **117**(3-4), 259-265.
- Lo Presti, D.C.F. (1989), *Proprietà Finamiche Fei Terreni*, in *XIV Conferenza Geotecnica di Torino*, Politecnico di Torino, Turin, Italy.
- Mayne, P.W. and Kulhawy, F.H. (1982), " $K_O$ - $OCR$  relationships in soils", *J. Geotech. Eng. Div.*, **108**(6), 851-872.
- Roesler, S.K. (1979), "Anisotropic shear modulus due to stress-anisotropy", *J. Geotech. Eng. Div.*, **105**(7), 871-880.
- Shibuya, S., Hwang, S.C. and Mitachi, T. (1997), "Elastic shear modulus of soft clays from shear wave velocity measurement", *Geotechnique*, **47**(3), 593-601.
- Skempton, A.W. (1986), "Standard penetration test procedures and the effects in sands of overburden pressure, relative density, particle size, ageing and overconsolidation", *Geotechnique*, **36**(3), 425-447.
- Tasiopoulou, P., Taiebat, M., Tafazzoli, N. and Jeremic, B. (2015), "On validation of fully coupled behavior of porous media using centrifuge test results", *Coupled Syst. Mech.*, **4**(1), 37-65.
- Yamashita, S., Kawaguchi, T., Nakata, Y., Mikami, T., Fujiwara, T. and Shibuya, S. (2009), "Interpretation of international parallel test on the measurement of  $G_{max}$  using bender elements", *Soil. Found.*, **49**(4), 631-650.
- Yang, J. and Gu, X.Q. (2013), "Shear stiffness of granular material at small strains: Does it depend on grain size?", *Geotechnique*, **63**(2), 165.
- Yoshimi, Y., Hatanaka, M. and Oh-Oka, H. (1978), "Undisturbed sampling of saturated sands by freezing", *Soil. Found.*, **18**(3), 59-73.
- Youn, J.U., Choo, Y.W. and Kim, D.S. (2008), "Measurement of small-strain shear modulus  $G_{max}$  of dry and saturated sands by bender element, resonant column, and torsional shear tests", *Can. Geotech. J.*, **45**(10), 1426-1438.
- Yu, P. and Richart, F. (1984), "Stress-ratio effects on shear modulus of dry sands", *J. Geotech. Eng. Div.*, **110**(3), 331-345.
- Zhang, W. and Goh, A.T. (2016), "Evaluating seismic liquefaction potential using multivariate adaptive regression splines and logistic regression", *Geomech. Eng.*, **10**(3), 269-280.